INTERNATIONAL JOURNAL OF
ENERGY AND ENVIRONMENT

Volume 5, Issue 2, 2014 pp.183-196
Journal homepage: www.IJEE.IEEFoundation.org

Inclusion of a simple dynamic inflow model in the blade element momentum theory for wind turbine application

Xiaomin Chen, Ramesh K. Agarwal

Department of Mechanical Engineering & Materials Science, Washington University in St. Louis, Campus Box 1185, One Brookings Drive, St. Louis, Missouri, 63130, USA.

Abstract
It is well established that the power generated by a Horizontal-Axis Wind Turbine (HAWT) is a function of the number of blades B, the tip speed ratio λ_r (blade tip speed/wind free-stream velocity) and the lift to drag ratio (C_L /C_D) of the airfoil sections of the blade. The previous studies have shown that Blade Element Momentum (BEM) theory is capable of evaluating the steady-state performance of wind turbines, in particular it can provide a reasonably good estimate of generated power at a given wind speed. However in more realistic applications, wind turbine operating conditions change from time to time due to variations in wind velocity and the aerodynamic forces change to new steady-state values after the wake settles to a new equilibrium whenever changes in operating conditions occur. The goal of this paper is to modify the quasi-steady BEM theory by including a simple dynamic inflow model to capture the unsteady behavior of wind turbines on a larger time scale. The output power of the wind turbines is calculated using the improved BEM method incorporating the inflow model. The computations are performed for the original NREL Phase II and Phase III turbines and the Risoe turbine all employing the S809 airfoil section for the turbine blades. It is shown by a simple example that the improved BEM theory is capable of evaluating the wind turbine performance in practical situations where operating conditions often vary in time.

Keywords: Wind energy; Horizontal-Axis; Wind Turbine; Blade momentum theory; In-flow model.

1. Introduction

Because of recent emphasis on carbon free renewable energy, there has been great deal of research directed towards the design of aerodynamically efficient wind turbines. There are mainly two kinds of wind turbines: Horizontal-Axis Wind Turbines (HAWT) and Vertical-Axis Wind Turbines (VAWT). Between them, HAWTs are the most commercially deployed turbines all over the world since they are able to generate more electricity at a given wind speed, especially in large wind farm applications when the wind is intermittent [1]. In a previous paper Chen and Agarwal [2] evaluated the effect of different airfoil sections on HAWT performance using the quasi-steady Blade Element Momentum (BEM) theory. This study focuses on modifying the quasi-steady BEM theory by including a simplified dynamic inflow model to capture the unsteady behavior of wind turbines on a larger time scale.

In order to calculate the wind turbine power, a Java-based aerodynamic analysis tool using Blade Element Momentum Theory has been developed based on Ceyhan's method [3]. The BEM analysis tool is validated against the field test data and Ceyhan's BEM results for two wind turbines: NREL (National

Renewable Energy Laboratory, USA) Phase II and III wind turbines. The NREL Phase II wind turbine has an untwisted and un-tapered blade while the NREL Phase III wind turbine has a twisted and un-tapered blade. Validations were performed to show the capabilities of our BEM analysis tool. The developed BEM tool is accurate and efficient in calculating the wind turbine performance based on comparisons with the test data.

The basic BEM theory assumes instant equilibrium of the wake when wind conditions change [4]. Therefore, it can be considered as the quasi-steady BEM (BEM^{qs}) theory. However, during operations of wind turbines in real situations, operating conditions such as wind speed, rotational speed, wind angle etc. often change depending upon the weather. Thus the wind turbine is not always in quasi-steady state. The simplified dynamic inflow model developed by Henriksen et al. [4] has been demonstrated to be capable of capturing the wind turbine performance due to changes in its operating conditions with time.

This paper incorporates this simplified dynamic inflow model into the quasi-steady BEM code (new code is denoted as BEM^{inflow}) and calculates the power generation of NREL Phase II and Phase III turbines and Risoe wind turbine described in Reference [3] at the starting stage of their operation when the rotational speed Ω changes from zero to its fully operational value. For the purpose of comparison, the wind speed of 12 m/s is chosen for all the three wind turbines; this wind speed is related to the rated power of Risoe wind turbine and is reasonable to consider in our analysis for NREL Phase II and Phase III turbines.

The airfoil section used in this study is S-809 [5] for NREL Phase II and Phase III wind turbines, and NACA 632xx series [6] for the Risoe wind turbine. Their aerodynamic characteristics, including C_L and C_D, are collected and expanded to a wider range of angles of attack for BEM calculation. The wind power calculation results using both BEM^{qs} and BEM^{inflow} are compared for a larger time period which is three times the one rotational period. It is shown that the simplified dynamic inflow model can successfully simulate the changes in wind turbine performance due to changes in wind conditions.

2. Brief overview of the blade element momentum (BEM) theory

This study employs Blade Element Momentum Theory for calculation of power output of a HAWT. The BEM theory models the axial and tangential induction factors by equating the force and torque relations for a small ring in the turbine plane (modeled as an actuator disk) derived from either the momentum theory or the blade element theory [7].

2.1 Momentum theory

In the momentum theory, we consider the stream tube surrounding the wind turbine which is modeled as an actuator disc as shown in Figure 1. Assuming steady, uniform, axisymmetric incompressible, inviscid flow with a nonrotating wake, the mass conservation in the stream tube gives the following relation:

$$\rho U_1 A_1 = \rho U_2 A_d = \rho U_4 A_4 \tag{1}$$

where A_d is area of the actuator disk.

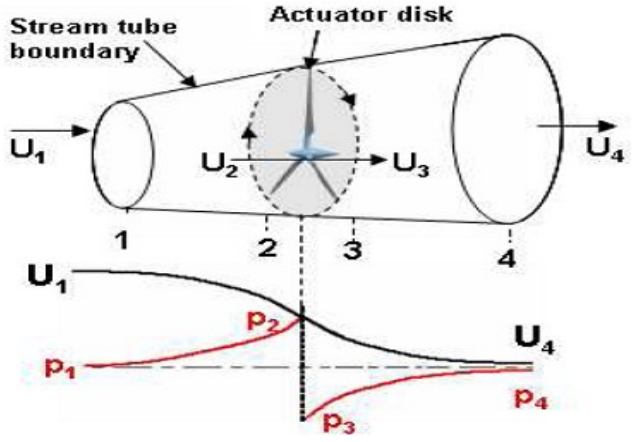

Figure 1. Actuator disk model of a wind turbine [6]

Since the actuator disc induces velocity in the stream tube, an axial induction factor *a* is defined as

$$a = \frac{U_1 - U_2}{U_1} \tag{2}$$

Thus, we have

$$U_2 = U_1(1 - a) \tag{3}$$

$$U_4 = U_1(1 - 2a) \tag{4}$$

Applying the Bernoulli equation between points 1, 2 and 3, 4, we can derive the following expression for pressure difference across the actuator disk:

$$p_2 - p_3 = \frac{1}{2}\rho(U_1^2 - U_4^2) \tag{5}$$

Thus, the net force normal to the plane on a ring of width *dr* in the actuator disk can be calculated as:

$$dN = (p_2 - p_3)dA_d = 4\rho U_1^2 a(1 - a)\pi r dr \tag{6}$$

Next, we consider the rotating annular stream tube shown in Figure 2.

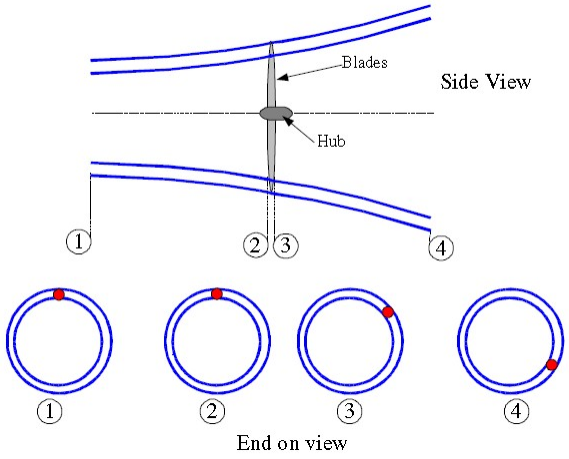

Figure 2. Rotating annular stream tube [6]

Defining an angular induction factor *a′* as:

$$a' = \frac{\omega}{2\Omega} \tag{7}$$

where ω is the angular velocity of the blade wake and Ω is the angular velocity of the blade, for a small elemental ring of width *dr* the torque can be obtained as:

$$dQ = \rho 2\pi r dr U_2 \omega r^2 \tag{8}$$

Using equation (7), the torque in equation (8) can be expressed as:

$$dQ = 4a'(1 - a)\rho U_1 \Omega r^3 \pi dr \tag{9}$$

2.2 Blade element theory

In the blade element theory, the blade is assumed to be divided into *N* sections which are called the blade elements. It is assumed that there is zero aerodynamic interaction between the blade elements and there is negligible span-wise velocity component on the blade. The forces on the blade element are solely determined by the lift and drag characteristics of 2D airfoils of the blade element; lift and drag components are defined perpendicular and parallel to the relative wind speed direction. The total tangential velocity experienced by the blade element is (1+ a') Ωr and the axial velocity is (1- a) U_∞. The relative wind velocity at the blade is given by:

$$W = \frac{U_\infty(1-a)}{\sin\phi} \tag{10}$$

The angle between the relative wind velocity and the plane of rotation is given by:

$$\tan\phi = \frac{U_\infty(1-a)}{\Omega r(1-a')} = \frac{(1-a)}{(1-a')\lambda_r} \tag{11}$$

where λ_r is the local tip speed ratio. The net force normal to the plane of rotation for each blade element and the resulting torque on each blade element can be written as:

$$dN = dL\cos\phi + dD\sin\phi \tag{12}$$

$$dQ = r(dL\sin\phi - dD\cos\phi) \tag{13}$$

where *dL* and *dD* are the lift and drag forces on the blade elements respectively. They are defined as:

$$dL = C_L\frac{1}{2}\rho W^2 c\,dr \tag{14}$$

$$dD = C_D\frac{1}{2}\rho W^2 c\,dr \tag{15}$$

For a multi-bladed wind turbine with *B* number of blades, one can write:

$$dN = B\frac{1}{2}\rho W^2(C_L\cos\phi + C_D\sin\phi)c\,dr \tag{16}$$

$$dQ = B\frac{1}{2}\rho W^2(C_L\sin\phi - C_D\cos\phi)cr\,dr \tag{17}$$

Defining the local solidity as $\sigma' = \frac{Bc}{2\pi r}$ and replacing W in equations (16) and (17) using equation (10), equations (16) and (17) become:

$$dN = \sigma'\pi\rho\frac{U_\infty^2(1-a)^2}{\sin^2\phi}(C_L\cos\phi + C_D\sin\phi)r\,dr \tag{18}$$

$$dQ = \sigma'\pi\rho\frac{U_\infty^2(1-a)^2}{\sin^2\phi}(C_L\sin\phi - C_D\cos\phi)r^2\,dr \tag{19}$$

2.3 Tip loss correction and modified BEM theory

The original BEM theory does not include 3D characteristics of the flow and viscous losses due to separation and turbulence. Some modifications have been applied to the theory to take into account these losses. The modified BEM theory includes the tip-loss and Glauert's corrections [8]. The tip-loss model

serves to correct the induced velocity resulting from the vortices shed from the blade tips into the wake on the induced velocity field while the hub-loss model corrects the induced velocity resulting from a vortex being shed near the hub of the rotor [8]. These losses are calculated by the equations:

$$F_{tip} = \frac{2}{\pi}\cos^{-1}\left(\exp\left(-\frac{B}{2}\frac{R-r}{r\sin\phi}\right)\right) \tag{20}$$

$$F_{hub} = \frac{2}{\pi}\cos^{-1}\left(\exp\left(-\frac{B}{2}\frac{r-r_{hub}}{r_{hub}\sin\phi}\right)\right) \tag{21}$$

The net tip loss is given by

$$F = F_{tip} * F_{hub} \tag{22}$$

The Glauert's empirical relation with a modification for the tip loss factor is given as:

$$C_T = \frac{8}{9} + (4F - \frac{40}{9})a + (\frac{50}{9} - 4F)a^2 \tag{23}$$

where

$$a = \frac{18F - 20 - 3\sqrt{C_T(50-36F) + 12F(3F-4)}}{36F - 50} \tag{24}$$

After considering tip loss and Glauert's correction, we obtain four equations - (25) and (26) derived from the momentum theory and (27) and (28) obtained from blade element theory as:

$$dN = 4F\rho U_1^2 a(1-a)\pi r dr \tag{25}$$

$$dQ = 4Fa'(1-a)\rho U_1 \Omega r^3 \pi dr \tag{26}$$

$$dN = \sigma'\pi\rho\frac{U_\infty^2(1-a)^2}{\sin^2\phi}(C_L\cos\phi + C_D\sin\phi)r dr \tag{27}$$

$$dQ = \sigma'\pi\rho\frac{U_\infty^2(1-a)^2}{\sin^2\phi}(C_L\sin\phi - C_D\cos\phi)r^2 dr \tag{28}$$

By equating the force relation (25) and (27) and torque relation (26) and (28), the axial induction factor a and the angular induction factor a' can be calculated. The process of calculating the induction factors is an iterative process shown in Figure 3. When the iteration converges, the induction factors can be determined which are then used to calculate the angles of attacks and thrust for each blade element separately; this information is then used for the wind turbine performance analysis. The total power from the rotor is given by:

$$P = \int_{rh}^{R} dP = \int_{rh}^{R} \Omega dQ \tag{29}$$

3. Simple dynamic inflow model

The BEM Theory discussed in section 2 is the basic quasi steady BEM Theory. It describes the steady state values of the induction factors and the pressure coefficient C_P and the thrust coefficient C_T. The aerodynamic model used in the basic quasi steady BEM Theory assumes instant equilibrium of the wake

when wind conditions change [4]. Therefore, we denote the axial induction factor a and the angular induction factor a' as a_n^{qs} and a_t^{qs} indicating their quasi-steady nature. In notation a_n^{qs}, 'n' denotes 'normal' meaning that it is an induction factor of the induced velocity normal to the rotor plane. In notation a_t^{qs}, 't' denotes 'tangential' meaning that it is an induction factor of the induced velocity tangential to the rotor plane. The corresponding induced velocities $v_n(r)$ and $v_t(r)$ are assumed to settle to their stationary values instantly [4], which can be described as follows:

$$v_n(r) = V_{rel} a_n^{qs}(\lambda, \theta, r) \tag{30}$$

$$v_t(r) = V_{rel} a_t^{qs}(\lambda, \theta, r) \tag{31}$$

where V_{rel} is the relative wind speed normal to the rotor plane.
A more realistic aerodynamic model is introduced in this section to capture the behavior of the wake behind an operating wind turbine by including a simple dynamic inflow model. Due to the existence of the wind turbine wake, the aerodynamic forces always settle to their new steady-state values after the wake settles to a new equilibrium whenever changes in the operating conditions occur [4]. In the simple dynamic inflow model due to Henriksen et al. [4], the tangential induced velocity is assumed to be quasi-steady given by equation (31). The induced axial or normal wind speed $v_n(r)$ is however computed by taking into account the variation in wind velocity with time. Let $\bar{v}_n(t)$ denote the averaged induced normal velocity with the temporal dynamics:

$$\tau_1 \dot{\bar{v}}_n + \bar{v}_n = V_{rel} \bar{a}_n^{qs}(\lambda, \theta) \tag{32}$$

where the time constant τ_1 satisfies the equation:

$$\tau_1 = \frac{1}{2} \frac{1.1R}{V_{rel} - 1.3\bar{v}_n} \tag{33}$$

In equation (33), R is turbine radius.
Solving equation (33) with the initial condition $\bar{v}_n(0) = 0$ gives the following solution:

$$\bar{v}_n(t) = \frac{V_{rel} \bar{a}_n^{qs}(\lambda, \theta) - \dfrac{10 V_{rel} \beta(t)}{13}}{\beta(t) - 1} \tag{34}$$

where

$$\beta(t) = \exp\left\{ V_{rel}(13\bar{a}_n^{qs}(\lambda, \theta) - 10) \left[\frac{2t}{11R} + \frac{\ln\left(1.3\bar{a}_n^{qs}(\lambda, \theta)\right)}{V_{rel}(13\bar{a}_n^{qs}(\lambda, \theta) - 10)} \right] \right\} \tag{35}$$

Thus, the induced axial (normal) wind speed states $v_n(r)$ can then be obtained as follows:

$$v_n(r) = \frac{a_n^{qs}(\lambda, \theta, r)}{\bar{a}_n^{qs}(\lambda, \theta)} \bar{v}_n \tag{36}$$

where

$$\bar{a}_n^{qs}(\lambda, \theta) = \frac{1}{R} \int_0^R a_n^{qs}(\lambda, \theta, r) dr \rangle 0 \tag{37}$$

The above assumptions and the simple inflow model are valid if the dynamic inflow is not very large. After all the tangential and axial induced wind velocity states are calculated, they are inserted into the procedure shown in Figure 3 for calculation of the aerodynamic performance of the wind turbine.
Because the tangential induced wind velocity is assumed to be quasi-steady and the normal induced wind velocity states $v_n(r)$ also depend on a_n^{qs}, the calculation of the influence of the inflow model first follows the basic BEM procedure shown in Figure 3 for calculation of the quasi-steady induction factors. Once the quasi-steady induction factors are computed, the influence of inflow model is computed using the procedure outlined in Figure 4. Figures 3 and 4 together form the complete procedure for the assessment of wind turbine performance using the BEM theory with simple dynamic inflow model.

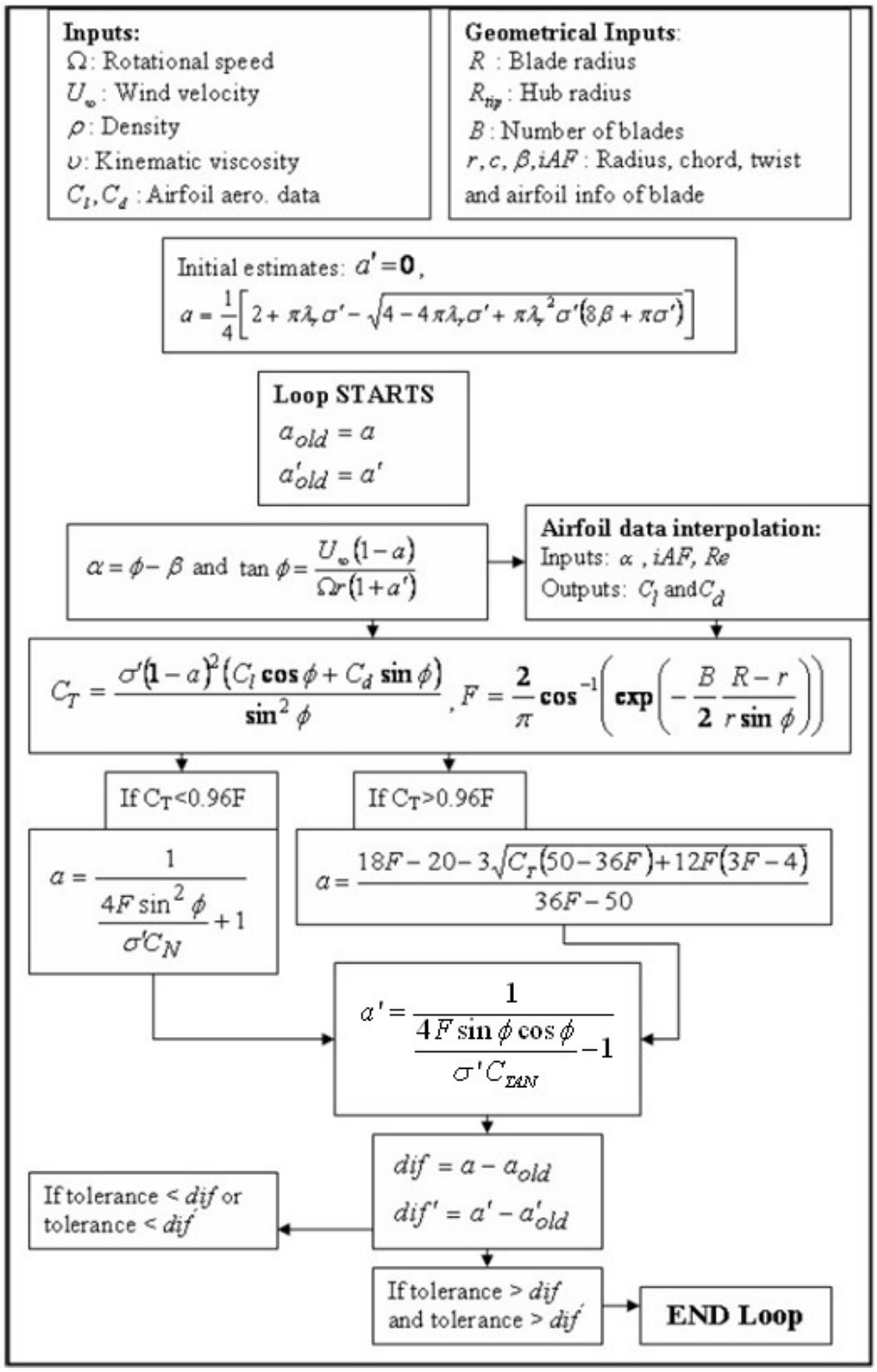

Figure 3. Iterative procedure for quasi-steady induction factors calculation

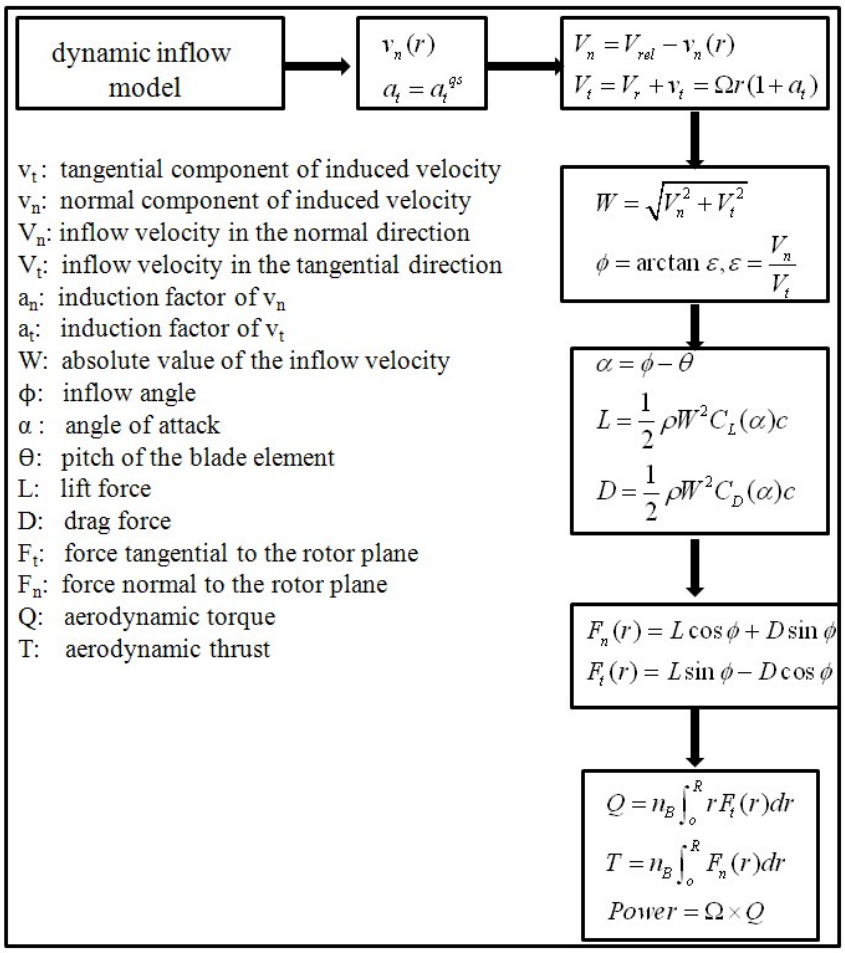

Figure 4. Procedure for calculation of the influence of dynamic inflow model

4. Airfoil data preparation

As shown in Figure 3, the iterative procedure for calculation of the induction factors requires the knowledge of aerodynamic characteristics (C_L and C_D) of the airfoils to determine the thrust coefficient C_T. This study employs the airfoil shapes that include S809 [5] and NACA 632xx series [6] airfoils. The experimental data for these airfoils is available in the open literature for a range of angles-of-attack (usually from -5 to 15 degrees) and Reynolds numbers [5, 6]. However, in the actual operation of a wind turbine, the blades experience very high angle-of-attack regimes. The currently available data needs to be expanded to cover high angles-of -attack regimes. This study uses Viterna's method in AirfoilPrep v2.2 developed by NREL [9] as the extrapolation tool to construct the C_L and C_D data between -180 and +180 degrees of angles of attack. The Reynolds numbers are chosen as some appropriate fixed numbers. Figure 5 shows an example of airfoil data extrapolation for DU 91-W2-250 airfoil.

5. Results and discussion

5.1 Validation of BEM^{qs} analysis tool

Before calculating the wind turbine power using the dynamic inflow model, BEM^{qs} code validations are performed to assess its accuracy and efficiency. Three different wind turbines are employed in the validation process. The calculated results are compared with the experimental data in Reference [5] and the BEM results of Ceyhan [3]. The first validation case is for the NREL wind turbine known as the NREL Phase II wind turbine which has untwisted and un-tapered blades. The wind turbine employs S809 airfoil section along the blade without any twist and taper. The operating conditions and geometrical properties are shown in Table 1 and Figure 6. The second validation case is for the NREL Phase III wind turbine which has twisted and un-tapered blades. Table 2 and Figure 7 provide the operating conditions and geometrical properties. The third validation case is for the Risoe wind turbine. This wind turbine has both twist and taper in the blades. In Risoe wind turbine, NACA 63-2xx series airfoils are used. Table 3 and Figure 8 provide the operating conditions and geometrical properties of Risoe wind turbine.

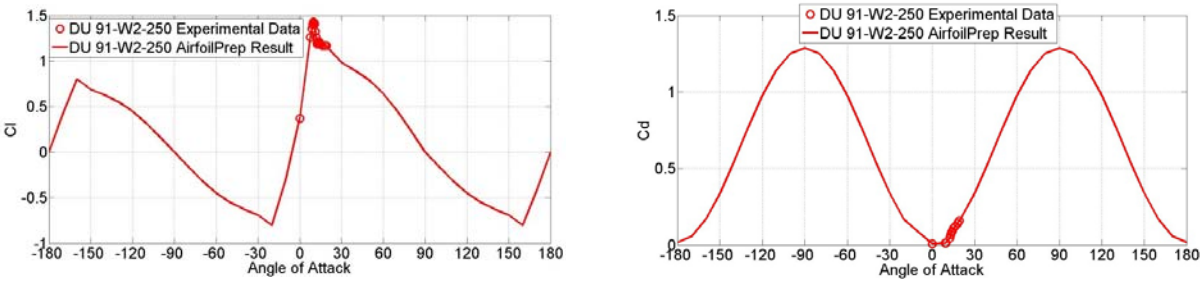

(a) Lift coefficient C_L (b) Drag coefficient C_D

Figure 5. Airfoil data extrapolation using the original experimental data

Table 1. NREL Phase II wind turbine general characteristics

Number of Blades	3
Turbine Diameter	10.06 m
Rotational Speed	71.3 rpm
Cut-in Wind Speed	6 m/s
Control	Stall Control
Rated Power	19.8 kW
Root Extension	0.723 m
Blade Set Angle	12 degrees
Twist	None
Chord	0.4572@all span location
Airfoil	S809

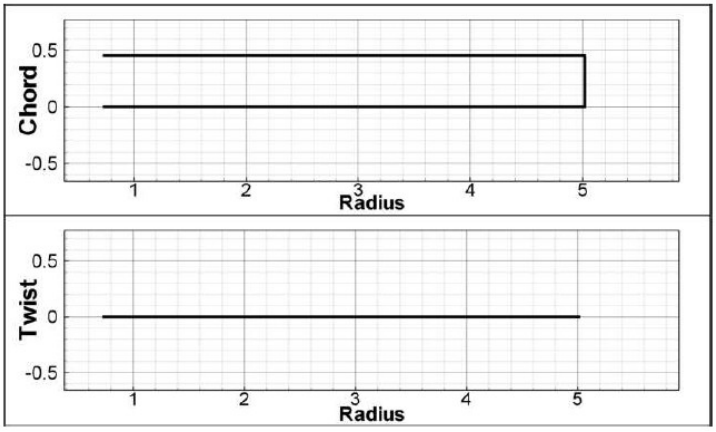

Figure 6. Geometric properties of NREL Phase II wind turbine

Table 2. NREL Phase III wind turbine general characteristics

Number of Blades	3
Turbine Diameter	10.06 m
Rotational Speed	71.3 rpm`
Cut-in Wind Speed	6 m/s
Control	Stall Control
Rated Power	19.8 kW
Root Extension	0.723 m
Blade Set Angle	3 degrees
Twist	44 degrees (max.)
Chord	0.4572@all span location
Airfoil	S809

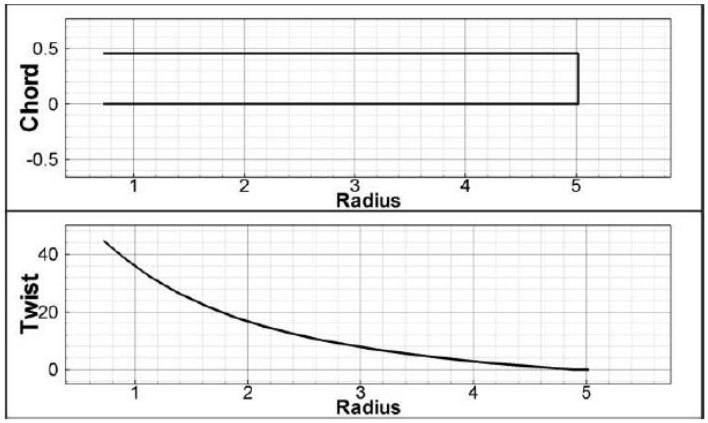

Figure 7. Geometric properties of NREL Phase III wind turbine

Table 3. Risoe wind turbine general characteristics

Number of Blades	3
Turbine Diameter	19.0 m
Rotational Speed	35.6 and 47.5 rpm`
Cut-in Wind Speed	4 m/s
Control	Stall Control
Rated Power	100 kW
Root Extension	2.3 m
Blade Set Angle	1.8 degrees
Twist	15 degrees (max.)
Root Chord	1.09 m
Tip Chord	0.45 m
Airfoil	NACA 63-2xx series

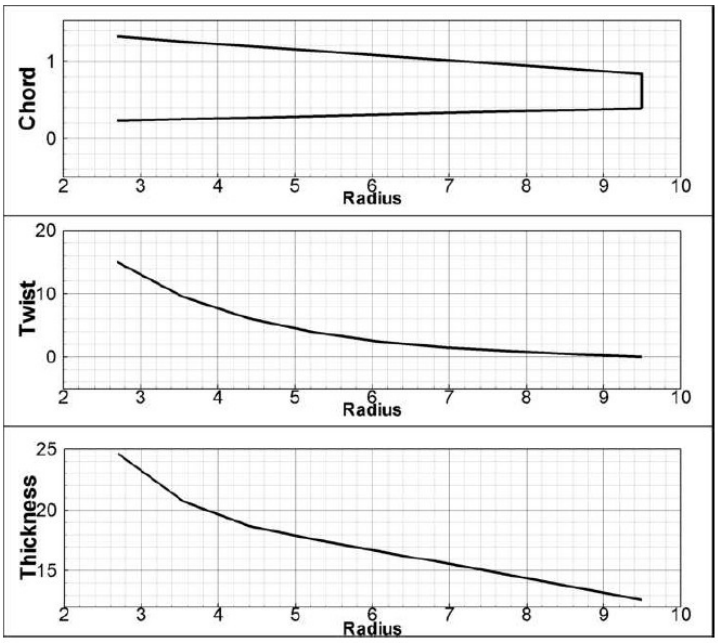

Figure 8. Geometric properties of Risoe wind turbine

Figures 9, 10 and 11 show the comparisons of results with the experimental data [5] and the computations of Cehyan [3] for NREL Phase II, NREL Phase III and Risoe wind turbines respectively. These three figures show that the BEM^{qs} analysis tool employed in this study performs quite well in

matching the experimental data for a wide range of wind speeds, especially at high wind speeds (greater than 8 m/s). The improvement in comparisons between the test data and computations at small wind speeds (lower than 8 m/s) requires more accurate C_L and C_D data. Considering that most large scale wind turbines operate at high wind speed, the validation results are acceptable and the BEM^{qs} analysis tool can be considered as a good code for estimating the power output from a wind turbine.

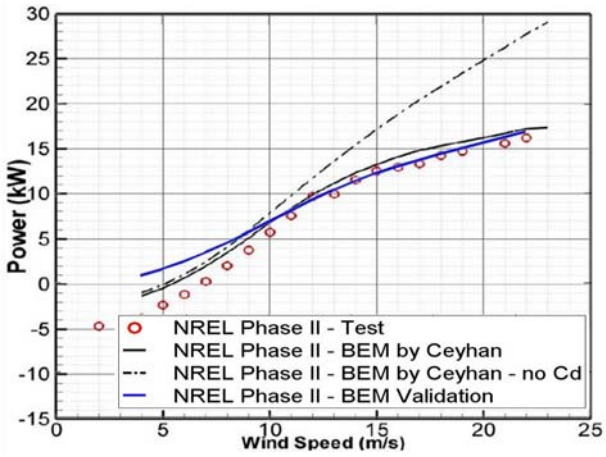

Figure 9. Comparison of BEM^{qs} calculations with test data for NREL Phase II wind turbine

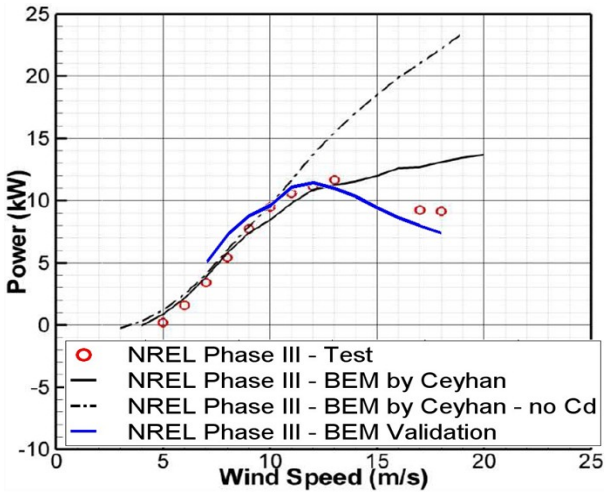

Figure 10. Comparison of BEM^{qs} calculations with test data for NREL Phase III wind turbine

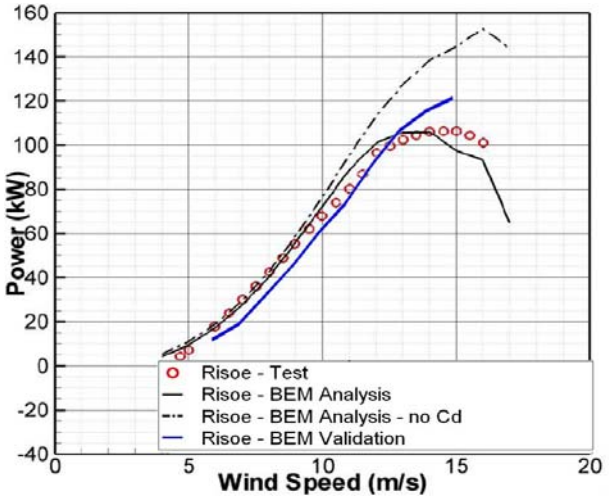

Figure 11. Comparison of BEM^{qs} calculations with test data for Risoe wind turbine

5.2 Inclusion of simple dynamic inflow model in BEM^{qs} (the code BEM^{inflow})

The simple dynamic inflow model described in section 3 is incorporated in BEM^{qs} code following the procedure outlined in Figure 4; the new code is designated as BEM^{inflow}. It can be employed to evaluate the influence of changes in wind speed and rotational speed of the rotor on power generation over a short time interval of interest due to intermittent wind conditions. We consider almost sudden change in the rotational speed of the rotor, a condition that always occurs during the startup stage of a wind turbine. The effect of this change in rotational operating condition at a fixed wind speed is simulated using the quasi-steady code BEM^{qs} and the BEM^{inflow} code that includes a simple dynamic inflow model. The power generated by the NREL Phase II, NREL Phase III and Risoe wind turbines is computed under this sudden change in rotational speed.

Again, the wind speed of 12 m/s is chosen as the mean steady wind speed for the three turbines; it is the wind speed used in calculating the rated power of Risoe wind turbine. We consider the startup stage of the wind turbines from zero rotational speed to desired rotational speed Ω (rad/sec) as given in Tables 1, 2 and 3. In addition to the free-stream wind speed, the input operating condition to the codes is the turbine rotational speed Ω which is provided as a time varying function. The changes in Ω with time during an initial time period of rotation *T* are shown in Figure 12 for NREL-Phase II and Phase III wind turbines, and in Figure 13 for Risoe wind turbine. Figures 14, 15 and 16 respectively show the output (power generation) from BEM^{qs} and BEM^{inflow} codes for NREL Phase II, NREL Phase III and Risoe turbines.

Figure 12 describes the starting stage of NREL Phase II and Phase III wind turbines at a fixed wind speed of 12m/s. The input rotational speed Ω changes from zero to the operating value of 71.3 rpm in a very short time. Figure 13 shows the change in rotational speed Ω for Risoe turbine from zero to the operating value of 47.5 rpm; the wind speed remains the same at 12m/s. Figures 14-16 show the change in output power generation of wind turbines due to almost sudden change in rotational speed. When Ω first reaches its operating value, the BEM^{qs} and BEM^{inflow} codes give slightly different results for power generation during the early stage where the effect of sudden change in Ω from zero to its operating value is to increase the power generation from the turbine for a very short period before it slowly goes back to its steady state value predicted by the quasi-steady BEM code BEM^{qs}.

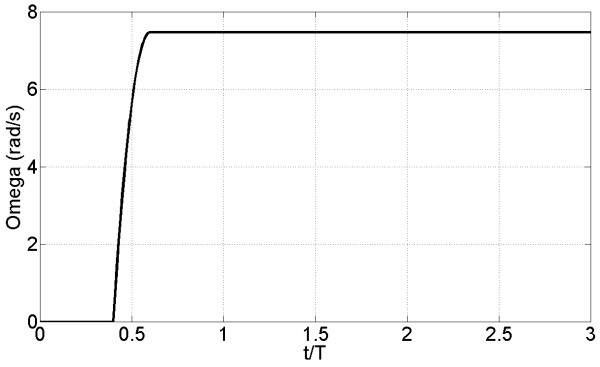

Figure 12. Input to BEM^{qs} and BEM^{inflow} codes for NREL Phase II and Phase III wind turbines

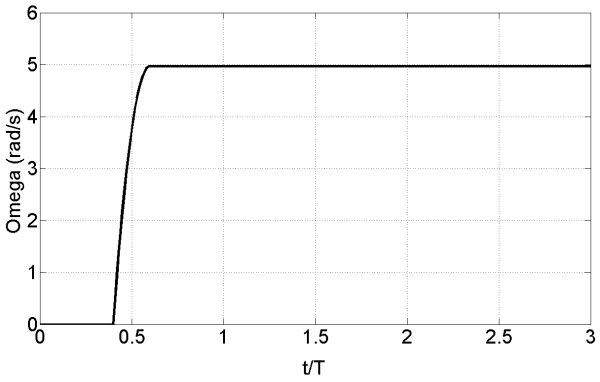

Figure 13. Input to BEM^{qs} and BEM^{inflow} codes for Risoe wind turbine

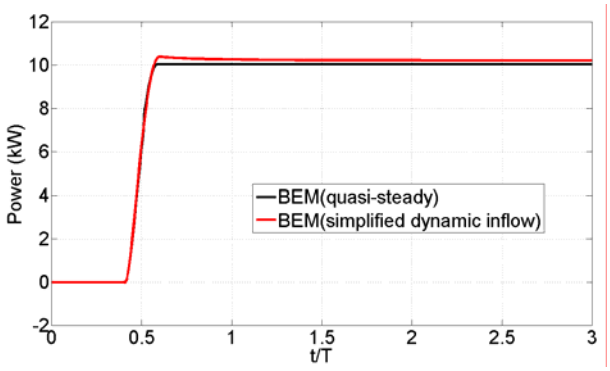

Figure 14. Output from BEM^{qs} and BEM^{inflow} codes for NREL Phase II wind turbine

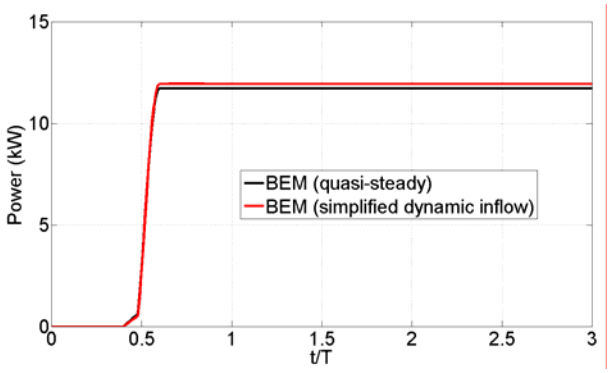

Figure 15. Output from BEM^{qs} and BEM^{inflow} codes for NREL Phase III wind turbine

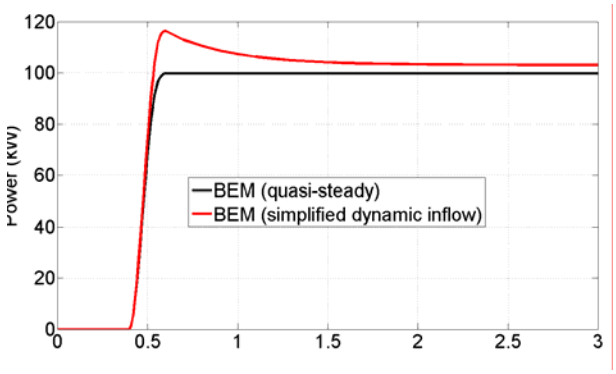

Figure 16. Output from BEM^{qs} and BEM^{inflow} codes for Risoe wind turbine

During the small time period when Ω changes from zero to its operating value, the BEM^{qs} code predicts the power increasing gradually with increase in Ω until it reaches the steady state value. BEM^{inflow} code however first predicts the power output higher than BEM^{qs} which then decreases slowly to the steady state value predicted by BEM^{qs}. This difference in the predictions of BEM^{qs} and BEM^{inflow} is due to the capability in BEM^{inflow} to account for sudden changes in flow conditions. Here we have only considered the effect of sudden change in rotational speed of the turbine. We have not considered the effect of changes in wind speed over certain time period; this aspect will be considered in our future work. This exercise is a demonstration of the effect of dynamic inflow in the rotor plane due to a change in its operating conditions.

6. Conclusions and future work

The primary focus of this study has been to modify the quasi-steady BEM theory by including a simple dynamic inflow model to capture the influence of unsteady wind conditions on the performance (power generation) of wind turbines on sufficiently large time scales of the order of a few hours. First, the quasi-

steady BEM code was validated by comparing its results with the experimental data available for NREL Phase II and Phase III turbines and the Risoe turbine. The quasi-steady BEM code was then modified to include a simple dynamic inflow model. The modified code was tested by considering the startup stage of wind turbines when their rotational speed increases from zero to the rated operational value; the free-stream wind speed was taken as a fixed value. The calculations showed that the modified BEM code predicts a higher value for power generation during the early stage compared to the prediction from the quasi-steady BEM code. The results show the need for including a dynamic inflow model in evaluating the performance of a wind turbine because of the intermittent nature of wind velocity. This paper has considered a very simple test case to show the effect of dynamic inflow in the rotor plane, the future work will consider the effect of changes in wind speed over a realistic time period.

Acknowledgement
The authors are grateful to Professor Ismail Tuncer of Middle East Technical University in Ankara, Turkey for providing the BEM code developed by his student O. Ceyhan.

References

[1] Energy-XS, "Vertical Axis Wind Turbines v/s Horizontal Axis Wind Turbines," accessed from http://www.energyexcess.com/node/7 (10 June 2010).
[2] Chen, X. and Agarwal, R., "Assessment of the Performance of Various Airfoil Sections on Power Generation from a Wind Turbine Using the Blade Element Momentum Theory," International Journal of Energy and Environment, Vol. 4, Issue 5, 2013, pp. 835-850.
[3] Ceyhan, O., Sezer-Uzol, N., and Tuncer, I.H., "Optimization of Horizontal Axis Wind Turbines by Using BEM Theory and Genetic Algorithm," Proc. of the 5th Ankara International Aerospace Conference, METU, Ankara, Turkey, 17-19 August, 2009.
[4] Henriksen, L.C., Hansen, M.H., and Poulsen, N.K., "A Simplified Dynamic Inflow Model and its Effect on the Performance of Free Mean Wind Speed Estimation," Wind Energy, 2012, doi: 10.1002/we.1548.
[5] Schepers, J. G. et al., "Final Report of IEA Annex XVIII: Enhanced Field Rotor Aerodynamics Database" Technical Report ECN-C-02-016, Energy Research Centre of Netherlands, Feb. 2002.
[6] Bertagnolio, F., Sørensen, N.N., Johansen, J., and Fuglsang, P., "Wind Turbine Airfoil Catalogue," Tech. Report No. Risø-R-1280(EN), Risø National Laboratory, Roskilde, Denmark, 2001.
[7] Ingram, G., "Wind Turbine Blade Analysis Using the Blade Element Momentum Method," Version 1.1, October 18, 2011.
[8] Moriarty, P.J. and Hansen, A.C., "Aerodyne Theory Manual," Technical Report No. NREL/TP-500-36881, January 2005.
[9] Viterna, L.A. and Janetzke D.C., "Theoretical and Experimental Power from Large Horizontal Axis Wind Turbines," NASA TM-82944, 1982.

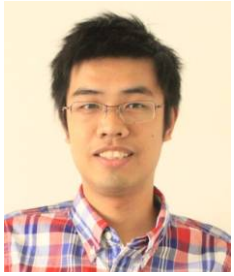

Xiaomin Chen is currently pursuing PhD in the Department of Mechanical Engineering & Materials Science at Washington University in St Louis. He received B.S. in Mechanical Engineering from Shanghai Jiao Tong University in China in 2008 and M.S. in Mechanical Engineering from Washington University in St. Louis in 2010. Xiaomin's research focuses on wind energy and aerodynamics. He is working on shape optimizations for wind turbine blades and optimization for wind-farm layouts using CFD method and genetic algorithms.
E-mail address: jackmin.chen@gmail.com

Ramesh K. Agarwal received the Ph.D degree in aeronautical sciences from Stanford University, Palo Alto, CA, USA in 1975. His research interests are in the theory and applications of computational fluid dynamics to study the fluid flow problems in aerospace and renewable energy systems. He is currently the William Palm Professor of Engineering in department of Mechanical Engineering and Materials Science at Washington University in St. Louis, MO, USA. He is a Fellow of ASME, AIAA, IEEE, and SAE.
Email address: rka@wustl.edu

